Modeling Anisotropic Interface Fracture Using Phase Field Cohesive Zone Approach in Composites

Modeling Anisotropic Interface Fracture Using Phase Field Cohesive Zone Approach in Composites

By
Dhaladhuli Pranavi and Amirtham Rajagopal

Cambridge
Scholars
Publishing

Modeling Anisotropic Interface Fracture Using Phase Field Cohesive Zone Approach in Composites

By Dhaladhuli Pranavi and Amirtham Rajagopal

This book first published 2025

Cambridge Scholars Publishing

Lady Stephenson Library, Newcastle upon Tyne, NE6 2PA, UK

British Library Cataloguing in Publication Data
A catalogue record for this book is available from the British Library

ISBN: 978-1-0364-1818-2
ISBN (Ebook): 978-1-0364-1819-9

Contents

Preface

Fracture is one of the major failure modes in structures, and computational modeling helps in understanding the crack initiation and propagation, which leads to ultimate fracture at various material length scales ranging from atomic to macroscales. At lower length scales, inhomogeneities exist that affect the mechanical and fracture response of the material at higher scales. Therefore, the interaction and effect of various material points on a particular point must be considered. This can be achieved by using nonlocal theories. According to Eringen's nonlocal theory, the stress at a point not only depends on strain at that point, but also on its neighborhood. Griffith's fracture criteria have been used, which state that the existing crack can propagate only when the energy release rate related to the extension of the crack reaches a critical value equal to the fracture toughness of the material. Of various computational models, phase field modeling (PFM) is one of the popular approaches to model fracture in cracking solids. The total energy is minimized with respect to the displacement field, which results in an equilibrium equation, and the evolution equation is derived based on dissipation and thermodynamic principles. The two governing equations are solved using a staggered approach to obtain the displacement field and crack phase field at each loading step.

Composites have been widely applied in various industries, as they can be modeled according to the required purpose, and can also provide high strength and stiffness at low weight. Accordingly, the fibers are embedded in the matrix constituent at various directions, due to which they become inherently inhomogeneous and anisotropic. The response of a composite system depends on the properties of the fiber, matrix, and fiber–matrix interface together with the stacking sequence and thickness of the laminate. Interaction of the crack with the fiber-matrix interface, and interfaces between different lamina in a laminate, play a key role in determining the overall strength of the system.

Cohesive zone models (CZM) frequently serve as the constitutive models for interfaces, linking the traction of the interface with its corresponding separation. The constitutive relation of the fracture at an interface is defined through a cohesive zone law, which is a traction-separation relation that represents the stress transmitted between the crack faces in a cohesive zone. The mechanical response of the composite system at micro-scale, having fiber, matrix, and fiber-matrix interface, can be considered to be isotropic. To model the fracture at micro-scale, a thermodynamically consistent phase field formulation for modeling the interactions between interfacial damage and bulk brittle fracture is presented in this thesis. A regularization scheme is considered for both the interface and the crack phase field. A coupled exponential cohesive zone law is adopted to model the interface, which has the contributions of both normal and tangential displacement jump components. A novel nonlocal approach is devised to evaluate the smoothened values of jump at the regularized interface using element-specific geometric information. Such a description of the interface allows a more realistic mechanical response of any composite system in terms of accurately representing failure modes such as matrix/bulk cracking, deflection and/or branching of crack at interface, through thickness penetration at interface, and delamination. The possibility of these would depend on modulus mismatch, inclination of the interface, length of the interface, and relative fracture toughness of the interface to the bulk. Several numerical examples are solved to validate the performance of the proposed model by peel test, crack interaction with an inclined interface, crack at a bimaterial interface, and stiff-soft

interface crack interaction.

Anisotropy can be broadly classified into (a) weak anisotropy, like transverse isotropy, orthotropy having one or two independent fiber orientations, and (b) strong anisotropy, like cubic symmetry, sawtooth crack patterns observed in thin anisotropic sheets. The weak or strong anisotropic systems can be defined from the polar plot of the inverse of orientation dependent fracture energy function. The composite system is anisotropic at meso and macro-scales, where a composite lamina having fibers embedded in matrix, or a composite laminate having different laminae stacked together is considered. Therefore, anisotropy is introduced into the elastic equilibrium by considering the distinct contributions of fiber and matrix in different modes. For simulating fracture in weakly anisotropic materials, like fiber reinforced composites having one or two fiber families, a convex fracture energy function is sufficient. A second-order structural tensor is introduced in the formulation, which acts on the gradient of the crack phase field. The crack driving force also constitutes distinct contributions of matrix and fiber constituents. To model the fracture in thin anisotropic sheets, where the crack path is unstable, and results in sawtooth type patterns and crack kinking, defining a non-convex fracture energy function is essential. A fourth-order structural tensor is introduced in a higher-order phase field approach to model strong anisotropy. Phase field model considering the interfacial damage for different configurations of a fiber reinforced composite is proposed and formulated. The crack and nonlocal interface are considered to be diffused. A coupled traction separation law based on a potential function is adopted to represent the behavior of the interface. The present model captures the predominant failure phenomena in a composite, such as matrix failure and delamination, by considering the role of fiber orientation, interface fracture properties and configuration of lamina. The proposed formulation is extended to a fiber reinforced composite lamina consisting of two fiber families oriented in different directions. Parametric studies are conducted to understand the effect of anisotropy parameter, length scales, fracture properties of fiber, matrix, and interface on crack propagation and mechanical response of the whole system. The two predominant failure modes in polycrystalline materials, namely, intergranular and transgranular fracture, occur based on the relative value of fracture toughness of the grain boundaries to that of the grains. The developed model is adopted to understand the transition between the two fracture phenomena. Numerical examples are performed to validate the proposed model, understand the anisotropic crack growth for unidirectional and woven fiber reinforced composites, study the interaction of anisotropic crack with composite-composite interface and metal-composite interface.

Certain composites, and elastomers are hyperelastic and anisotropic in nature and, in general, subjected to mixed mode loading rather than pure modes. Soft biological tissues can also be considered anisotropic hyperelastic material. A thermodynamically consistent anisotropic phase field formulation for modeling the mixed mode fracture of hyperelastic materials like rubber, silicone elastomers, fiber reinforced composites, and soft biological tissues at finite strains is proposed and formulated. In this work, an equivalent crack surface energy density function considering volumetric-deviatoric split, and tension-compression split is adopted. A coupled Neo-Hookean model with orthotropic anisotropy, which is suitable for modeling fiber reinforced composites, and soft biological tissues, is considered. Phase field method is adopted to model the complex crack initiation, and propagation in the materials, by considering a single damage variable. The proposed model is validated by conducting fracture tests on (a) natural rubber reinforced with black carbon, (b) silicone elastomers, (c) unidirectional fiber reinforced composites, and (d) brain tissue reinforced with axons. The results obtained are compared with the experimental and numerical investigations present in the existing literature.

About the Author

Dr. D. Pranavi is a lead engineer at GE Aerospace, India. She has completed her doctorate (PhD) and masters (M. Tech) under the guidance of Prof. Amirtham Rajagopal, Department of Civil Engineering, IITH. She has completed her bachelors (B.Tech) from JNTUH college of Engineering Hyderabad. Her research interests include fracture mechanics, cohesive zone modeling and mechanics of composites. She has 5 international journal publications, 7 international conference publications, and 1 book chapter.

Prof. A. Rajagopal is a professor at the Department of Civil Engineering, IITH. He is the recipient of DST Young Scientist Fellowship Award, 2012. Damage mechanics, fracture mechanics, multiscale modeling of materials, mechanics of composites, linear/nonlinear finite element method, meshless methods, polygonal FEM, and phase field approach are some of his research interests.

Contributors

Dr. Preethi Kasirajan
Department of Civil Engineering
Indian Institute of Technology Hyderabad
Telangana
India

Dr. Karthik S
Assistant Professor
Department of Civil Engineering
Dayananda Sagar College of Engineering
Karnataka
India

I would like to extend my sincere thanks to Prof. J. N. Reddy and Prof. Arun Srinivasa, Texas A&M University, USA, and Prof. Paul Steinmann, Universität Erlangen–Nürnberg, Erlangen, Germany, for their valuable insights and productive discussions.

Symbols

Ω	Solid body
Ω_{m}	Matrix
Ω_{inc}	Inclusion
Ω_{o}	Reference/undeformed configuration
Ω_{t}	Current/deformed configuration of the body at time t
$\mathscr{G}_c$	Griffith's critical energy release rate
$\mathscr{G}_c^{\mathrm{I}}$	$\mathscr{G}_c$ associated with the interface
$\mathscr{G}_c^{\mathrm{iso}}$, $\mathscr{G}_c^{\mathrm{m}}$	$\mathscr{G}_c$ of matrix constituent of the composite material
$\mathscr{G}_{cI}^{\mathrm{iso}}$, $\mathscr{G}_c^{\mathrm{mI}}$	Mode I $\mathscr{G}_c$ of matrix constituent of the composite material
$\mathscr{G}_{cII}^{\mathrm{iso}}$, $\mathscr{G}_c^{\mathrm{mII}}$	Mode II $\mathscr{G}_c$ of matrix constituent of the composite material
$\mathscr{G}_c^{\mathrm{ani}}$, $\mathscr{G}_c^{\mathrm{f}}$	$\mathscr{G}_c$ of fiber constituent of the composite material
$\mathscr{G}_c(\theta)$	Orientation dependent critical fracture energy function
$\boldsymbol{\sigma}$	Cauchy stress tensor
$\boldsymbol{\varepsilon}$, $\overline{\boldsymbol{\varepsilon}}$	Strain tensor
$\boldsymbol{\varepsilon}^{\mathrm{e}}$	Bulk local strain tensor
$\boldsymbol{\varepsilon}^{\mathrm{j}}$	Nonlocal regularized strain tensor
$\boldsymbol{\sigma}^{nl}$	Nonlocal stress tensor
ρ	Density of the material
ε^{nl}	Nonlocal strain tensor
$\underline{\mathbf{u}}$	Displacement field
$\overline{\mathbf{b}}$	Body force field per unit volume
$\overline{\mathbf{t}}$	Traction on the boundary of the continuum
E	Total energy functional
E_{s}	Strain energy
E_{c}	Fracture energy
E_{I}	Energy corresponding to the interface
$\mathsf{E}_{\mathrm{ext}}$	Energy due to external forces
F	Free energy functional
Ψ_{e}, g_0	Elastic energy density
Ψ_{e}^{+}	Tensile part of the elastic energy density
Ψ_{e}^{-}	Compressive part of the elastic energy density
Ψ_{o}	Elastic energy density of the undamaged solid
$\Psi_{\mathrm{o}}^{\mathrm{iso}}$	Ψ_{o} of matrix constituent of the composite material
$\Psi_{\mathrm{o}}^{\mathrm{ani}}$	Ψ_{o} of fiber constituent of the composite material
Ψ_{I}	Strain density function associated with the interface
Ψ_{v}	Volumetric contribution of the elastic energy density
Ψ_{d}	Deviatoric contribution of the elastic energy density
Γ	Sharp crack surface
Γ_ϕ	Regularized crack surface functional
Γ_{I}	Sharp interface
Γ_α	Regularized interface functional

ϕ	Phase field parameter
η	Non conservative order parameter
α	Interface order parameter
l_ϕ	Phase field length scale parameter
l_α	Interface field length scale parameter
$g(\phi)$	Degradation function
k	Small positive constant
λ	Lame's first parameter
μ	Lame's second parameter
μ_f	Stress like material parameter related to fibers
$\mathbf{n}$	Outward normal to surface boundary
$\mathscr{H}$	History parameter
υ	Viscosity parameter
P_I	I^{th} node
V_I	Voronoi polygon
$V_{\underline{\mathbf{x}}I}$	Second order Voronoi polygon
$\mathbf{C}$, $\mathbb{C}$	Fourth order constitutive tensor
κ	Coefficient of gradient energy
E	Young's modulus
E_1, E_2	Young's muduli along principal ply directions of a composite (2D)
G_{12}	shear moduli in 1-2 plane of a composite (2D)
ν	Poisson's ratio
ν_{12}	ν with loading in the 1 direction and strain in the 2 direction
θ	Crack orientation
ξ	Fiber orientation
ζ	Angle of tearing
$\mathscr{B}$, $\mathscr{A}$	Second order structural tensor
$\mathbb{B}$	Fourth order structural tensor
$\mathbf{I}$	Second order identity tensor
$\mathbb{I}$	Fourth order identity tensor
$\mathbf{a}$	Unit vector corresponding to the fiber orientation
β	Anisotropy parameter
$\mathbf{T}$	Transformation matrix
φ	Angle of material axis
$\mathbf{H}_\phi$	Hessian matrix
$\boldsymbol{\varkappa}$	History parameter
$\mathbf{t}$	Traction vector
$\mathbf{j}$	Displacement jump vector
j^n	Displacement jump component in normal direction
j^t	Displacement jump component in tangential direction
t^n	Traction component in normal direction
t^t	Traction component in tangential direction
t_u^n	Cohesive strength corresponding to mode *I*
t_u^t	Cohesive strength corresponding to mode *II*
$\mathbf{X}$	Material point
$\mathbf{x}$	Spatial point
$\mathbf{a}_0$	Orientation vector in reference confirguration
$\mathbf{a}$	Orientation vector in spatial confirguration
$\mathbf{F}$	Deformation gradient
$\mathbf{C}$	Right Cauchy–Green tensor

$\mathbf{b}$	Left Cauchy–Green tensor
$\underline{J}$	Volume ratio
$\underline{\mathbf{F}}$	Deviatoric component of deformation gradient
$\underline{\mathbf{C}}$	Deviatoric component of Right Cauchy–Green tensor
$\mathbf{P}$	First Piola–Kirchhoff stress tensor
$\mathbf{S}$	Second Piola–Kirchhoff stress tensor
v_f	Volume fraction

Chapter 1

Introduction

1.1 Failure

Failure represents the breakdown of the material (such as metal, concrete or plastic) due to various factors that affect the strength, stability, and chemical composition of the material's structure. Failure characterizes the functioning or lack of functioning of the material to its desirable or intended requirement. Some of the common causes of failure are

- Yielding
- Buckling
- Fatigue
- Fracture
- Creep
- Impact
- Corrosion
- Damage

Damage is a physical discontinuity in the object or material. It can be introduced either during manufacturing or service stage. The damage can impair the usefulness or normal functioning of the object or material. The damage can be of micro, meso and/or macro scale. Damage characterizes the state of the object or material. The quantitative evaluation of damage location, shape, size, evolution and effect can be performed based on experimental, analytical and numerical techniques [1].

Fracture is the separation of an object or material into two or more pieces under the action of applied/induced stress. Fracture strength, or breaking strength, is the stress when a specimen fractures [1].

1.1.1 Fracture Mechanics

The assumption that macro cracks preexist in materials is inherent to fracture mechanics. It assumes that failure starts at these preexisting macro-cracks. Two new surfaces are created in a thermodynamically irreversible manner when the fracture propagates. The fracture process on a macroscopic scale may be roughly classified as brittle fracture and ductile fracture. In brittle fracture, the irreversible work associated with a fracture is confined to a negligibly small process zone adjacent to

the crack surfaces, while the remaining material is deformed elastically. Therefore, cracks can pass easily through brittle materials. On the contrary, ductile fracture involves a large amount of plastic deformation in a significant process zone adjacent to the crack surfaces. The ductile fracture process absorbs a large amount of energy, and thus cracks do not pass easily through ductile materials. Materials that behave in a ductile manner under normal conditions can sometimes become brittle under some special conditions. For example, steel becomes brittle at low temperatures. A thick plate made of ductile material may allow brittle cracks to grow in the portion that is deep inside, away from the free surfaces. Linear Elastic Fracture Mechanics (LEFM), a subfield of fracture mechanics, deals with fracture problems where the size of the process zone is negligibly small. The elastic material response throughout the fracture process is assumed. LEFM can only be applied to the brittle fracture process. In this work, brittle fracture is modeled using LEFM principles.

Modes of Fracture

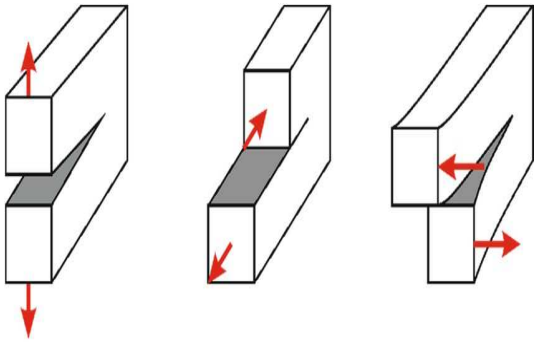

Figure 1.1: Figure: (a) Mode *I*, (b) Mode *II* and (c) Mode *III*.

There are three independent crack opening modes. They depend on the relationship between the direction of the loading and the direction of the fracture surfaces.

- Opening mode *I* occurs when tensile loading is applied perpendicular to the fracture surfaces.
- Sliding mode *II* occurs when in-plane shear loading is applied in the direction parallel to the fracture surfaces.
- Tearing mode *III* occurs when out of plane shear loading is applied in the direction parallel to the fracture surfaces.

Crack opening modes are presented pictorially in Figure 1.1. Any crack can be viewed as the superposition of these three basic modes.

1.1.2 Griffith's criterion

Griffith's theory [12] is based on energy balance on a global scale. Consider a deformable body with an embedded sharp crack of area A. The body is under arbitrary loading. The law of conservation of energy states

$$\dot{P} = \dot{\mathsf{E}}_s + \dot{\mathsf{E}}_k + \dot{\mathsf{E}}_f \tag{1.1}$$

$\dot{P}$ is the work performed by the applied loads per unit time. $\dot{\mathsf{E}}_s$ and $\dot{\mathsf{E}}_k$ are the rates of change of internal energy and kinetic energy of the body. $\dot{\mathsf{E}}_f$ is the energy spent in increasing the crack area per unit time. E_f is the fracture energy necessary to create a new fracture surface when the crack propagates. It is expressed as

$$\mathsf{E}_f = \mathscr{G}_c A \tag{1.2}$$

$\mathscr{G}_c$ is a material parameter called Griffith's critical energy release rate. It is the energy necessary to create a unit area of the new fracture surface. It should be noted that $\mathscr{G}_c$ does not depend on the geometry of the body. Kinetic energy can be neglected if the applied loads are time-independent, and if the crack growth is slow. Equation 1.1 can be modified as

$$\frac{\partial \Pi}{\partial t} + \frac{\partial \mathsf{E}_f}{\partial t} = 0 \tag{1.3}$$

$\Pi = \mathsf{E}_s - P$ is the potential energy of the body. Change in crack size brings about all the changes in time, and therefore, the following relation holds.

$$\frac{\partial}{\partial t} = \dot{A}\frac{\partial}{\partial A} \tag{1.4}$$

Using Equation 1.4, we can rewrite Equation 1.3 as follows

$$\left(\frac{\partial \Pi}{\partial A} + \frac{\partial \mathsf{E}_f}{\partial A}\right)\dot{A} = 0 \tag{1.5}$$

The term $\frac{\partial \Pi}{\partial A}$ represents the energy available for crack growth and can be referred to as the crack driving force. It is denoted by the symbol $\mathscr{G}$ in honor of Griffith. The term $\frac{\partial \mathsf{E}_f}{\partial A}$ represents the resistance of the material that must be overcome for crack growth, and it equals to $\mathscr{G}_c$. Therefore, we write

$$\left(\mathscr{G}_c - \mathscr{G}\right)\dot{A} = 0 \tag{1.6}$$

For a crack to grow (i.e., $\dot{A} > 0$), $\mathscr{G}$ should exceed $\mathscr{G}_c$. Therefore, the criterion for crack initiation in a body is

$$\mathscr{G} = \mathscr{G}_c \tag{1.7}$$

This theory is incapable in predicting the nucleation of crack. In order to overcome this, a variational framework of Griffith's theory based on energy minimization is introduced by Francfort et al. [2]. Phase field modeling (PFM) has been developed using variational approaches [3]. This enables the simulation of complex fracture phenomena involving crack branching and crack merging.

A plate with an edge crack is shown in Figure 1.2. In this case, three zones can be presumed to be present. First, a stress free zone where there is a formation of a traction free surface classified as a strong discontinuity resulting in a sharp traction jump. Second is the cohesive zone, where the separation is resisted by the cohesive traction's, having a region of weak discontinuity and a region ahead of the crack tip, where the microcracking, void initiation, propagation, and fusion takes place, which is characterized by a smooth jump. The length of this region constitutes the fracture process zone. The zone ahead of the crack tip where all micro-mechanisms are active is the nonlocal region. The cohesive forces present in the fracture process zone must be considered, especially when the characteristic lengths are comparable with length scale of the material. Cohesive zone models are originated by treating fracture phenomena as gradual where the dissolution takes place near the extended crack tip (cohesive zone) as depicted in Figure 1.2. Traction forces occur in the normal and the shear directions.

A cohesive law is a traction-separation relation that represents the stress transmitted between the crack faces in a cohesive zone. The relation is such that, across the interface, with an increase in the separation, the traction increases, reaches a peak value, decreases, and then eventually ceases. In structural applications of composites, failure/damage mostly happens under mixed-mode loading rather than pure modes. Under pure modes (Mode *I*, Mode *II* and/or Mode *III*), the onset of failure can be obtained by comparing the traction components of each mode with their respective allowable

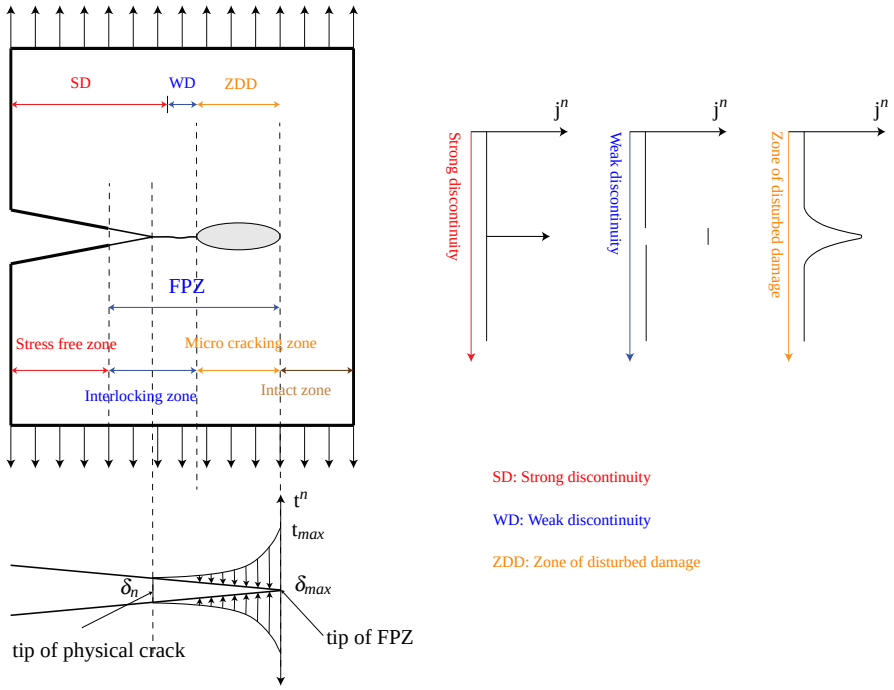

Figure 1.2: Phenomenological description of a quasi-brittle fracturing process in a cohesive model.

critical values at an interface. However, under mixed-mode condition, both normal and tangential components are transferred at the interface, and the onset of failure occurs when any one or both of the traction components (normal, shear) involved reach their respective allowable values.

Different forms of cohesive laws exist such as polynomial, linear, and exponential among others. In this work, exponential law is followed; such a definition allows us to have derivatives which are continuous, and is beneficial in a computational scheme. Independent cohesive laws have been defined for the mixed-mode case, where the normal and tangential components of traction and/or separation have no interaction or coupling (see [4] and [5]). To model the realistic interface behavior, a coupling between the modes is considered [6]. The dependence of the fracture toughness on mode ratio is accounted for through quadratic criterion as [7]:

$$\left(\frac{\mathscr{G}_I}{\mathscr{G}_{IC}}\right)^2 + \left(\frac{\mathscr{G}_{II}}{\mathscr{G}_{IIC}}\right)^2 = 1 \tag{1.8}$$

1.2 Failure of composites

Composites are naturally occurring or engineered materials with two or more constituent phases. Composites have advantageous structural properties such as tailored material properties to suit the design, high stiffness, and strength, among others. They are used widely in several important industrial applications. To enable efficient design of such composites, it is important to understand the complex failure mechanisms in such materials [8]. There exists an interface between the constituent phases of a composite material. Interfaces can be either due to a direct bonding between the two constituent phases or due to an adhesive that bonds the two phases. In this case, the adhesive constitutes an *interphase*. The interface significantly affects the mechanical characteristics of the composite material and is responsible for the load transfer between the constituent phases. These composites are predominantly quasi-brittle in nature and are prone to failure by either a fracture and/or damage. At various stages of loading, nucleation and growth/coalescence of voids/micro cracks into macro voids/cracks occur at locations of stress concentration.

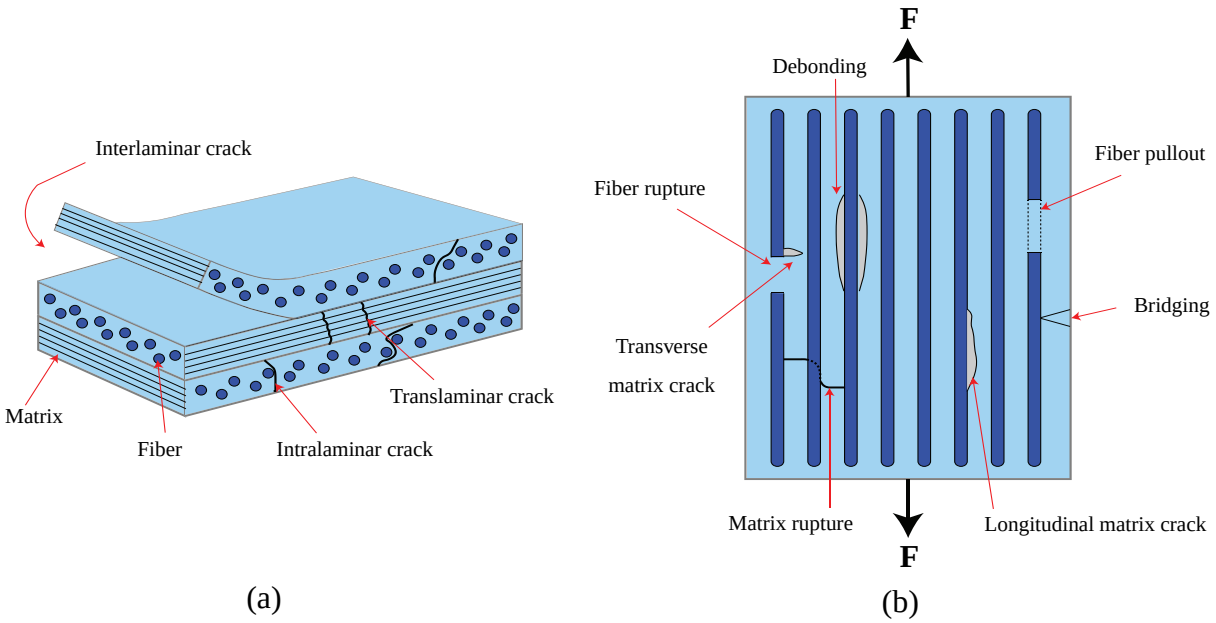

Figure 1.3: Schematic diagram of (a) failure modes in a fiber reinforced composite laminate and (b) fiber and matrix cracks in a composite lamina.

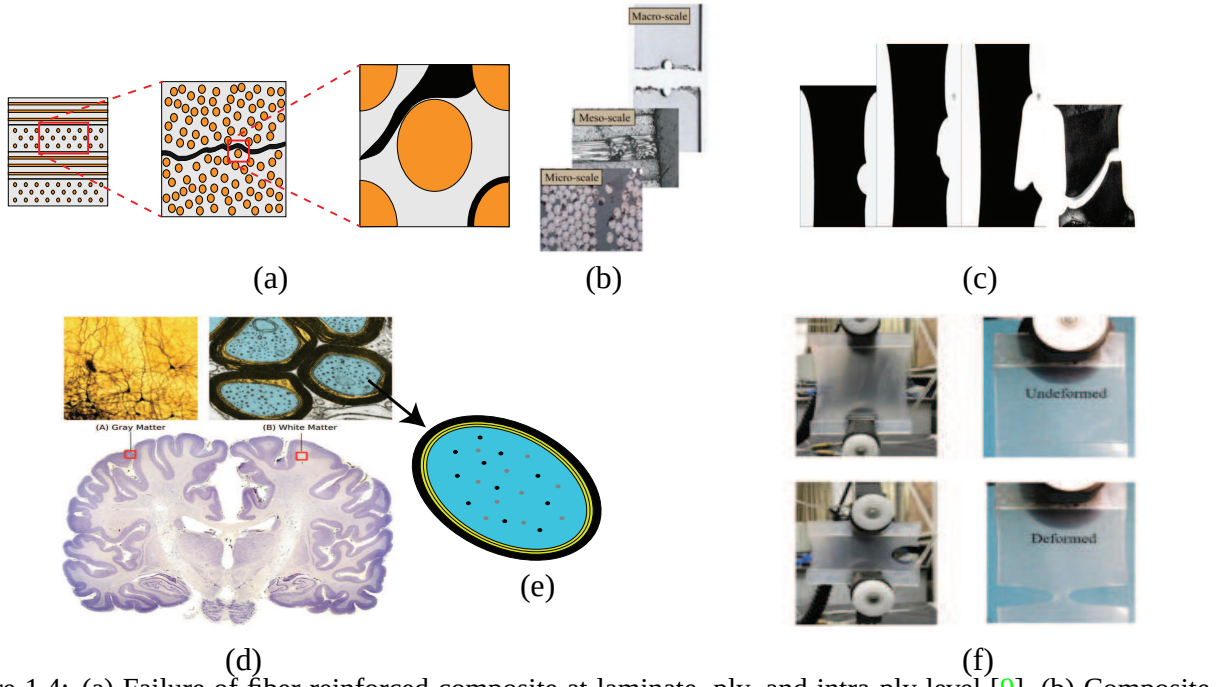

Figure 1.4: (a) Failure of fiber reinforced composite at laminate, ply, and intra-ply level [9], (b) Composite damage at different length scales [10], (c) Crack propagation in a carbon black-filled rubber [11], (d) Grey and white matter of the brain [12], (e) Illustration of the arrangement of the myelin sheath (black boundary) and the axon in cross-section (black dots: microtubules; grey dots: neurofilaments), and (f) Experimental photos of pure shear test and DENT test of silicone rubber [13].

The interaction and subsequent clustering of macroscopic cracks leads to their propagation with the formation of new surfaces and ultimately failure. The anisotropic material behavior of FRCs makes it more complex to model. The properties of different constituent phases, namely fiber, matrix, fiber-matrix interface, together with the stacking sequence and thickness of the laminate, determine the overall properties of such composites. Interaction of the interfaces is a crucial factor in

determining the overall strength of the composite [14]. Failure modes of a laminated fiber-reinforced composite at mesoscale can be distinguished broadly into: (a) *Intralaminar*, failure within the lamina like matrix cracking or fiber breakage; (b) *Interlaminar*, failure between the laminae like delamination; and (c) *Translaminar*, failure along the laminate thickness, as shown in Figure 1.3 [15].

In some fiber reinforced composites, elastomers, and soft biological tissues, inherent inhomogeneity and anisotropy coexist, and they behave elastically when subjected to large deformations. The failure in certain anisotropic materials under large deformations is depicted in Figure 1.4.

1.3 State of Art

According to Eringen's theory of nonlocal elasticity [16, 17], the stress $\boldsymbol{\sigma}$ at a reference point $\mathbf{x}$ depends on the strain field at that point $\mathbf{x}$, and also on the strain field of the points $\mathbf{x}'$ in the neighbourhood of $\mathbf{x}$. The size of the neighbourhood region is associated with a length scale parameter τ which acts as a localization limiter. When the dependence of the strain field is expressed in a differential form, the nonlocality is a case of strong nonlocal theory, and when the dependence of the strain field is expressed in an integral form, then it is a case of weak nonlocality.
The linear nonlocal elasticity model for homogeneous and isotropic elastic solids is given by

$$\boldsymbol{\sigma}^{nl}_{kl,k} + \rho\,\left(\bar{\mathbf{b}}_l - \ddot{\mathbf{u}}_l\right) = 0 \tag{1.9}$$

Where,

$$\boldsymbol{\sigma}^{nl}_{kl}(\boldsymbol{x}) = \int_V \alpha\left(|\mathbf{x}' - \mathbf{x}|, \tau\right)\,\boldsymbol{\sigma}_{kl}(\mathbf{x}')\,d\mathrm{V}(\mathbf{x}') \tag{1.10}$$

$$\boldsymbol{\sigma}_{kl}(\mathbf{x}') = \lambda\,\boldsymbol{e}_{rr}\,\mathbf{x}'\,\delta_{kl} + 2\,\mu\,\boldsymbol{e}_{kl}\,\mathbf{x}' \tag{1.11}$$

$$\boldsymbol{e}_{kl}(\mathbf{x}') = \frac{1}{2}\left[\frac{\partial\,\mathbf{u}_k(\mathbf{x}')}{\partial\,\mathbf{x}'_l} + \frac{\partial\,\mathbf{u}_l(\mathbf{x}')}{\partial\,\mathbf{x}'_k}\right] \tag{1.12}$$

Where $\boldsymbol{\sigma}^{nl}_{kl}$ is the stress tensor, ρ is the density, $\boldsymbol{f}_l$ is the body force and $\mathbf{u}_l$ is the displacement vector at point $\mathbf{x}$ at time t; $\boldsymbol{\sigma}_{kl}(\mathbf{x}')$ is the classical stress tensor related to strain, $\boldsymbol{e}_{kl}(\mathbf{x}')$ at point $\mathbf{x}'$ and at time t. $\alpha\left(|\mathbf{x}' - \mathbf{x}|, \tau\right)$ is the kernel function, $\tau = e_o a/l$, where e_o is the material constant, a and l are internal and external characteristic lengths respectively. For a special class of kernels, these integro-partial differential equations can be reduced to a set of singular partial differential equations. These models have been extensively used in literature (see [18–27]).

Remark1: The properties of the nonlocal modulus or kernel function α can be listed as (i) α is a delta sequence, (ii) For small a, $\tau \to 1$, the nonlocal theory approximates atomic lattice dynamics, (iii) α can be determined by matching the dispersion curves of plane waves with those of atomic lattice dynamics (or by performing experiments) for a given material, and (iv) α can be generalized in such a way that the integrals over the domain of integration should give unity. The nonlocal elasticity in the limit $\tau \to 0$ reverts to classical elasticity [16, 17].

Remark2: Anisotropy is considered to be two-fold: (a) anisotropy of the elastic moduli tensor, and, (b) anisotropy of the nonlocality. The anisotropy and nonlocality are described through nonlocal elastic moduli and nonlocal kernel function. This is generally expressed in terms of the Hessian matrix in the lattice approaches [28]. For isotropic solids, the nonlocal kernel function $\alpha(\mathbf{x}' - \mathbf{x})$ which brings the influence of the strain fields in the neighboring directions, is spherical in range with center $\mathbf{x}$, whereas, for anisotropic materials, it may, in general, attenuate at different rates in different directions [29]. Eringen's nonlocal elasticity can be adopted for anisotropic materials by

using a special Gaussian kernel having two length scales [30] and by using nonlocal kernels, which are the Green functions of the Helmholtz equation in nonlocal isotropic elasticity [17]. A three-dimensional nonlocal anisotropic kernel has been derived using Erigen's nonlocal anisotropic model that captures anisotropic length scale effects.

A note on the use of Eringen's nonlocal theory for the analysis of functionally graded beams, plates, and shells is presented in [31]. The properties of the nonlocal modulus and its dependence on the internal length scale are brought out. The use of Eringen's nonlocal model with different nonlocal approaches is discussed with evidence from the literature. The following conclusions are drawn.

- Eringen's nonlocal model is applicable for homogeneous and isotropic material in three dimensions. The kernel function has a meaning of nonlocal modulus that reduces to elastic properties with a limiting value on the length scale.
- For two-dimensional structural elements where the material is inhomogeneous through the thickness (only), the following comments apply:
  - The anisotropy of the elastic moduli tensor and anisotropy of the nonlocality can be described using nonlocal elastic moduli and nonlocal kernel function [28].
  - Through-thickness FGM beams, plates, and shells can be modeled using Eringen's nonlocal model [27]. Nonlocal kernel function similar to Eringen's model is adopted. Nonlocality in elastic moduli is considered using homogenization theories such as the rule of mixtures or Mori–Tanaka methods [32].
  - An equivalent strain definition can be used to define the nonlocal nature of the strain. This will allow defining a modified Eringen nonlocal model as [33]

$$\varepsilon_{ij}^{nl} = \int_V \alpha\left(|\mathbf{x}' - \mathbf{x}|, \tau\right) \varepsilon_{ij}(\mathbf{x}')\, d\mathrm{V}(\mathbf{x}')$$

    The above definition only accounts for the nonlocality in kernel function.
  - A fourier frequency domain analysis can be carried out and nonlocal material moduli can be obtained by considering lattice dynamics and nonlocal elasticity models along with experimental data [34].
  - Nonlocal fractional derivative models are also useful for materials with varying material properties [35].
- The nonlocal elasticity in the limit $\tau \to 0$ reverts to classical elasticity [16].

The phase field method (PFM) [2] has emerged as one of the best methods for solving problems with interfaces. The total potential energy of cracking solids [3] is minimized to obtain both displacement field and crack set simultaneously. A variational framework for rate-independent and viscous over-force models is proposed in [36] and [37]. Phase field approach combined with natural neighbor Galerkin method is used to model fracture in quasi-brittle materials [38] and for the evolution of composition [39]. The PFM is also used for predicting damage in transient dynamic analysis (see [40] and [41]). Ductile fracture is modeled using PFM in a 2D framework in [42]. Fracture in anisotropic solids can also be modeled [43].

Cohesive zone models are often used as the interface constitutive models relating the interface traction with its corresponding separation. Earlier works by Dugdale [44] and Barenblatt [45] on the cohesive zone model are notable. The spread of the discrete/sharp interface into a narrow transition layer between the two phases results in a diffused interface. The physical properties change smoothly across the interface. The diffused interface involves an additional order parameter in the context of phase transition. The introduction of one or more parameters helps in overcoming the need to

solve for a definite location of the interfacial surface at each loading step, which results in a better understanding of physics in the interface region [46]. The application of diffused models for the interface phenomena is implemented by van der Waals [47], Landau and Ginzburg [48], Cahn and Hilliard [49]. Some of the examples are dendritic solidification (see [50] and [51]), phase transition phenomena [52], pure substances [53], TJs (Triple Junctions), interfaces in binary alloys (see [54] and [55]), metal solidification and grain growth (see [56] and [57]), and liquid-liquid interface [58]. The diffused model is an asymptotic to sharp model when the interface width is considered to be zero. In the biomechanics field, for modeling arteries, bones (mineral and collagen), and dental implantology, the interface is more often considered to be diffused. Based on the type of implant used for integrating into the bone, the interface can be considered sharp or diffused. The interface is sharp when an inert material like titanium is implanted and it is assumed to be diffused for bioactive materials like bioglass. Of the two, the bioactive material can be better integrated [59]. The diffused interface model combines the advantages of the phase field approach and the cohesive zone model and results in modeling mesh-independent crack nucleation and growth along arbitrary paths.

1.4 Objectives of the book

The book focuses on nonlocal models for isotropic and anisotropic materials, which can capture weak or strong anisotropy at small and finite strains. The aim is to understand the crack-interface interaction at different material length scales in fiber-reinforced composites, polycrystalline materials, and can be applied to any material-having interfaces. Practically, all of the structural elements are subjected to mixed mode loading; therefore, developing a nonlocal model that can capture the mode-mixity is essential. The objectives of the present research work are:

1. To model crack propagation in isotropic materials using phase field approach:
    - To use a mesh-free natural neighbor Galerkin method for phase field modeling of the fracture problems for isotropic materials.
    - To develop a thermodynamically consistent phase field model for damage by defining a non-conservative order parameter that represents the damage.
2. To model anisotropic fracture using phase field approach:
    - To study the different sources of anisotropy and the factors classifying anisotropy into weak and strong anisotropy.
    - To understand the influence of orientation-dependent fracture energy on the crack propagation.
    - To introduce anisotropy into the elastic equilibrium and crack driving force to understand the overall response of the system.
    - To model anisotropic fracture in materials like, fiber reinforced composites, and thin polymeric sheets.
3. To model crack-interface interaction in isotropic materials using phase field and cohesive zone approaches:
    - To model the mechanical response of the material using a strain energy density function by considering tension-compression split.
    - To model the fracture at the interface using a coupled traction separation law.
    - To model the interaction between the crack propagation and interfacial damage at small strain.

4. To model crack-interface interaction in anisotropic materials using phase field and cohesive zone approaches:
    - To extend the phase field-cohesive zone approach to model the intraction of anisotropic crack propagation with interfacial damage.
    - To understand and study the influence of anisotropy parameters and orientation dependent fracture energy on the failure of composite laminates and polycrystalline materials.
5. To model anisotropic mixed-mode fracture in hyperelastic materials:
    - To model the microscopic response of natural rubber reinforced with carbon black fibers, and fiber-reinforced composites.
    - To model the mixed-mode fracture in soft silicone elastomers.
    - To study the anisotropic response of brain under different loading conditions.

1.5 Outline of the book

In chapter 2, a mesh-free natural neighbor Galerkin method is presented for phase field modeling of the fracture problems and demonstrated through numerical experiments like, a plate with an embedded center crack and an edge notched specimen under tension. A thermodynamically consistent phase field model is developed for damage by defining a non-conservative order parameter that represents the damage. Modified Crisfield Arc-length method and staggered approach algorithm for solution are presented. In chapter 3, the weak and strong anisotropy is discussed and demonstrated by modeling fracture in composites, and polymeric sheets. In chapter 4, a nonlocal phase field approach together with cohesive zone model is proposed to demonstrate the crack-interface interaction. Various cracking events like crack branching, deflection/penetration, and delamination at the interfaces are discussed. In chapter 5, we present a phase field-cohesive zone approach to understand the influence of anisotropy parameter, length scales, and configuration of lamina on the response of the composite system. The occurence of the two fracture events in polycrystalline materials, namely, intergranular and transgranular fracture, is studied. Chapter 6 deals with modeling of mixed-mode fracture in elastomers, understanding the anistropic response of soft biological tissues. The summary of the present research work and the scope for the future study are presented in chapter 7.

Chapter 2

Phase Field Modeling of Fracture/Damage in Brittle and Quasi-Brittle Materials

2.1 Introduction

Computational modeling of damage or fracture process in materials is a challenging task in solid mechanics. The failure of material involves its degradation due to nucleation and growth of micro defects, such as voids and cracks, which coalesce to form a macro defect. Modeling strategies offer cost-effective predictive solutions under realistic conditions, compared to full-scale experimental studies. Continuum Damage Mechanics (CDM) [60] describes the measure of material degradation on a micro-scale and then reflects the average material degradation on the macro-scale by use of damage variables [61]. This helps to develop models which can predict material behavior more accurately. The degradation in material properties can be looked upon as a mode of failure and is identified with a damage variable. This process of material degradation could also result in the formation of new surfaces, i.e., cracks at micro-scale or macro-scale identified as fracturing of the material. In contrast to damage mechanics, which mainly deals with the microdefects and their evolution, fracture mechanics deals with the macroscopic cracks of finite length.

Fracture in solids can be modeled by using a continuous or a discontinuous approach (also referred to as a discrete approach). CDM and smeared crack models are the widely used theories associated with the continuous approach for fracture. Linear Elastic Fracture Mechanics (LEFM) [62] and Cohesive Zone Models (CZM) [63] are widely used theories associated with the discontinuous approach for fracture. The application of these concepts to discrete/smeared approaches in a numerical setting requires additional criteria for crack initiation and propagation [31, 64]. Also, dynamic fracture requires a criteria to describe crack branching [65]. A study and comparison of various crack propagation criteria is done in [66] and [67]. In addition, it is observed that numerical modeling of localization phenomena such as fracture, shear band formation, plasticity, moving interfaces, and phase transformations requires some form of adaptive mesh refinement. These result in computationally expensive and mesh-dependent results [68]. CDM-based formulations have been developed in numerical modeling of material degradation and fracture in strain-softening types of materials. In these formulations, it has been shown that the formulation lacks a characteristic length scale, and the results are found to be mesh-dependent. To overcome these, various regularization theories have been developed and reported in the literature such as viscous regularization theories [69], Cosserat theories [70], Non-local continuum theories [71], Gradient enhanced damage model [72] and Gradient damage model [73].

The recent advances have been towards developing non classical continuum theories that regularize the solution and incorporate a characteristic length scale for modeling localized phenomena such as damage or fracture that could have inbuilt criteria for onset of damage or fracture and result in mesh-independent crack or damage paths in a numerical setting. Phase field models [74, 75],

Peridynamic approaches [76] and Lattice models [77], Molecular dynamics approaches [78] have been popular in recent times. Each of these methods has applicability over a particular length scale; for instance, phase field models are valid from micron-scale to macro-scale. The major advantage of phase field and peridynamic models is that the crack paths are automatically determined as part of the solution, and they can handle complex fractures such as crack branching and intersections.

The phase field methods are thermodynamically consistent variational approaches that allow evolution of microstructure, that has multiple phases and trace the transformations between these phases [79]. The general applications of the phase field approach can be seen in damage and fracture, microstructure evolution [56], interfaces [80], anisotropy [81], phase transformations [82], grain growth simulation [83] and even bioapplications [84]. Bourdin et al. [85] developed the first phase field model (PFM) based on the variational approach for brittle fracture, which was extended from Griffith's fracture theory [62] where the sharp crack was regularized by a damage band due to the introduction of a scalar phase field that differentiated the damaged and undamaged material. The free energy functional of the Ginzburg-Landau type in the material is minimized during the evolution of these variables [56]. In phase field methods, the microstructure of the material is represented by the field variables termed as order parameters, which are either conserved (for instance, in composition) or non conserved (for instance, in damage or fracture). This method is truly nonlocal in the sense that, unlike sharp interface models, the field variable or order parameter is diffused or regularized and defined over a finite width length scale. During the energy minimization process, the evolution of the conserved field variable or order parameter results in the Cahn-Hilliard equation [79] whereas the non-conserved field results in the Allen-Cahn equation [86]. The phase field equations are nonlinear partial differential equations of second or fourth order having spatial and time derivatives. Analytical solutions to these equations are difficult to obtain, and hence numerical solutions are generally resorted to in problems such as brittle crack propagation [75], quasi-brittle fracture [87], damage and fatigue [88], dynamic fracture [89], ductile fracture [90] and even coupled temperature-rate dependent fracture [91]. A few literature review papers on the phase field models for brittle, quasi-brittle and ductile fracture in quasi-static and dynamic loads implemented in the framework of the finite element method are presented by Wu et al. [92], Ambati et al. [93], Bourdin et al. [85], Spatschek et al. [94] and Del Piero [95]. Rabczuk [96] presented an extensive overview of popular computational methods for modeling brittle fracture. The stability analysis of the phase field method for fracture for a generic degradation function can be seen in [97]. The numerical solution consists of spatial and time discretization. Spatial discretization is done by using standard finite difference [98], finite element [99], mesh free [100], and/or spectral methods [101] as any domain shape and boundary conditions can be considered. Time integration is done either in implicit [75], explicit [102] and/or semi-implicit approaches [103].

Phase field was first developed in the context of variational approach to brittle fracture by Francfort and Marigo [2] which is considered to be an approximation, whereas the regularized version of Bourdin et al. [74] is itself a model and referred to as an isotropic second-order phase field fracture model. This isotropic model was extended by Amor et al. [104] for an anisotropic version where the elastic energy was decomposed into the volumetric and deviatoric parts to prevent cracking in compression. Freddi and Royer-Carfagni [105] unified the formulations of Bourdin et al. [74], Amor et al. [104], and Lancioni and Royer-Carfagni [106] for mode *I*, mode *II*, mixed-mode, and masonry-like fractures. Borden et al. [107] proposed a fourth-order phase field model that improves the convergence rates of the numerical solution. This is shown to be a special case of Li et al. [108] surface anisotropic phase field model. A $\mathscr{C}^1$ continuous isogeometric finite element was considered for these higher-order models [109]. A model similar to Bourdin's was presented by Kuhn and Muller [110]. Miehe et al. [99] presented a phase field fracture model based on geometry, continuum mechanics, and a thermodynamic basis. A quadratic function was adopted in all these phase field models for the crack surface density function where the range of phase field is admissible i.e, $\phi \in [0,1]$ for the resulting exponential distribution of phase field, but this choice regularizes the sharp

crack into a diffuse crack with infinite supports. Due to this, the evolution equation has to be solved at every point in the domain to determine the phase field value. Also, the linear elastic behavior before the onset of damage is not easy to deal with as damage is initiated right at the beginning. Hence, Pham et al. [73] proposed a non-standard phase field model consisting of a linear crack density surface function resulting in a diffuse localization band with parabolic distribution of phase field and exhibiting the initial linear elastic stage. But the range of the phase field will not be admissible, and the boundedness of it should be explicitly enforced [111]. Tanne et al. [112] claim that a strict positive elastic limit is a necessary condition for the correct prediction of crack nucleation in phase field models. Wu [87] proposed a phase field model valid for both brittle and quasi-brittle fractures where a generic crack surface density function was presented. Later, Wu [113] presented a simpler alternate formulation for the phase field model. As an alternate for anisotopic formulation where the equilibrium equation is nonlinear leading to computational inefficiency, a hybrid phase field formulation was considered [93] [114] where the equilibrium equation was linearized and assymetric tension/compression behavior is captured without any loss of computational cost. In the hybrid models, the crack patterns remain the same as in anisotropic models, but the load-displacement graph slightly differs.

2.2 Phase field model for brittle fracture

Any numerical strategy for the implementation of the phase field model should address the issue of the smoothness of approximation required to accurately capture the distribution of the phase field parameter over the regularized region defined by a suitable limiting length scale parameter. In a limiting sense, the diffused interface model must reduce to a sharp interface model at very low values of the length scale. There have been some recent works on the use of meshless methods for the implementation of phase field models of fracture. For instance, element free Galerkin method [115] and consistent meshless methods [116] have been proposed. In section 2.2, the issues related to the need for finer mesh near the crack path and the accuracy of the solution are addressed. Therefore, a mesh-free natural neighbor Galerkin method is used for phase field modeling of the fracture problems. The notion of using natural neighbors to dynamically decide the compact support at a nodal point renders it truly mesh-free and nonlocal. The method uses smooth non-polynomial type Sibson interpolants, which are $\mathscr{C}^0$ at a given node and $\mathscr{C}^\infty$ everywhere. This allows the accurate capture of the interface region in a phase field model with fewer nodes compared to the standard finite element method. For the required accuracy, the cost of computation from the natural neighbor Galerkin method is almost equal to the finite element method. For the same quadrature, the mesh-free method gives more accurate results.

2.2.1 Thermodynamically consistent nonlocal phase field model for brittle fracture

Let us consider a continuous body $\Omega \in \mathbb{R}^d (d \in 1,2,3)$ with the sharp crack $\Gamma \in \mathbb{R}^{\delta-1}$ as shown in Figure 2.1. Let $\mathbf{u}(x,t)$ be the displacement of any material point at $x \in \Omega$ at any time $t \in \mathbb{R}$. Consider $\bar{\mathbf{b}}$ as the body force field per unit volume and $\bar{\mathbf{t}}$ as the tractions on the boundary $\partial\Omega_t$. In 1920, Griffith [62] laid out the theoretical foundation for brittle fracture. Griffith's theory suffers from limitations such as the inability to predict crack nucleation and identify complex crack paths. These limitations are overcome by the variational framework of Griffith's theory introduced by Francfort et al. [117]. The process of crack initiation and propagation in the body is governed by the minimization of the total energy functional written as

$$E(\mathbf{u},\Gamma) = E_s + E_c - E_{ext} \tag{2.1}$$

E_s, E_c and E_{ext} are the strain energy, fracture energy, and energy due to external forces written as

$$\mathsf{E}_s = \int_\Omega \Psi_e(\boldsymbol{\varepsilon})\ d\Omega, \quad \mathsf{E}_c = \int_\Gamma \mathscr{G}_c\, d\Gamma, \quad \mathsf{E}_{ext} = \int_\Omega \bar{\mathbf{b}}\cdot\mathbf{u}\, d\Omega + \int_{\partial\Omega_t} \bar{\mathbf{t}}\cdot\mathbf{u}\, dA \tag{2.2}$$

Ψ_e is the elastic energy density and $\mathscr{G}_c$, a material parameter known as Griffith's critical energy release rate, is the energy required to create two new fracture surfaces. This minimization problem is referred to as a free discontinuity problem [118]. It should be noted that the crack path Γ and the displacement field $\mathbf{u}$ (discontinuous across Γ) are not known a priori.

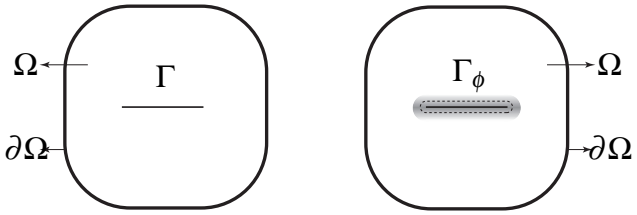

(a) (b)

Figure 2.1: (a) Sharp crack Γ embedded in the body Ω and (b) Regularized crack surface Γ_ϕ.

Phase field approximation for a sharp crack

We implement the free discontinuity problem by introducing a phase field $\phi(\mathrm{x},\mathrm{t})$ for the description of a sharp crack Γ in a solid continuum Ω. Its value at any material point varies between 0 and 1 ($\phi = 0$ and $\phi = 1$ representing undamaged and fully damaged phases, respectively). The phase field $\phi(\mathrm{x},\mathrm{t})$ captures the onset and development of micro-voids and micro-cracks in a macroscopically homogeneous body. Bourdin et al. [119] presented the regularized variational framework of Griffith's theory to study the diffused crack propagation. The sharp crack Γ is regularized with the functional Γ_ϕ as

$$\Gamma_\phi = \int_\Omega \gamma(\phi,\nabla\phi)\, d\Omega, \quad \gamma(\phi,\nabla\phi) = \frac{1}{2l_\phi}\left(\phi^2 + l_\phi^2 |\nabla\phi|^2\right) \tag{2.3}$$

where, $\gamma(\phi,\nabla\phi)$ is the crack surface energy density function per unit volume of the solid as given by Miehe et al. [120]. The length scale l_ϕ governs the width of the crack, i.e., it governs the region where ϕ transitions from 1 to 0. It is to be noted that for vanishing length scales $l_\phi \to 0$, the regularized crack functional Γ_ϕ converges to the sharp crack Γ ($\Gamma_\phi \to \Gamma$). For any sharp crack Γ in the body, the regularized crack phase field $\phi(\mathrm{x})$ can be obtained by minimizing the functional Γ_ϕ with respect to ϕ, subject to the Dirichlet type condition $\phi = 1$ on the sharp crack Γ. The Euler equations for the minimization problem is given as $\phi - l_\phi^2 \Delta phi = 0$ along with the Neumann type boundary condition $\nabla\phi\cdot\mathbf{n} = 0$ on $\partial\Omega$. This is demonstrated using a numerical example in the Section 2.4.2. Using the crack surface density function $\gamma(\phi,\nabla\phi)$ given in eq. (2.3), the fracture energy E_c can now be written as

$$\mathsf{E}_c = \int_\Gamma \mathscr{G}_c\, d\Gamma = \int_\Omega \mathscr{G}_c\, \gamma(\phi,\nabla\phi)\, d\Omega \tag{2.4}$$

Governing equations

Since the phase field $\phi(\mathrm{x},t)$ is smeared, the degradation of the elastic energy density with increase in the phase field should be accounted for. Therefore, the strain energy of the body is written as

$$\mathsf{E}_s = \int_\Omega \left[(1-\phi)^2 + \mathsf{k}\right] \Psi_e(\boldsymbol{\varepsilon})\, d\Omega, \quad \Psi_e(\boldsymbol{\varepsilon}) = \frac{1}{2}\lambda\ \mathrm{tr}^2(\boldsymbol{\varepsilon}) + \mu\ \mathrm{tr}(\boldsymbol{\varepsilon}^2) \tag{2.5}$$

where, λ and μ are Lame's constants. k is a small positive constant which ensures a small artificial stiffness of $\mathsf{k}\Psi_e(\boldsymbol{\varepsilon})$ at a fully broken state of $\phi(\mathrm{x},\mathrm{t}) = 1$. The expression for strain energy of the body as written in eq. (2.5) facilitates crack growth under compression, which is an unrealistic response. To ensure the crack growth only under tension, only tensile part of the elastic energy should be degraded with the increase in the phase field. Therefore, the strain energy of the body is given as

$$\mathsf{E}_s = \int_\Omega \left[(1-\phi)^2 + \mathsf{k}\right] \Psi_e^+(\boldsymbol{\varepsilon})\, d\Omega + \int_\Omega \Psi_e^-(\boldsymbol{\varepsilon})\, d\Omega \tag{2.6}$$

Ψ_e^+ and Ψ_e^- are defined as given by Miehe et al. [120] on the basis of the spectral decomposition of the strain tensor as $\boldsymbol{\varepsilon} = \sum_{i=1}^{\delta} \varepsilon^i \mathbf{n}^i \otimes \mathbf{n}^i$, where ε^i and $\mathbf{n}^i$ are principal strains and principal strain directions. Using this, we write $\boldsymbol{\varepsilon}_\pm = \sum_{i=1}^{\delta} \langle \varepsilon^i \rangle_\pm \mathbf{n}^i \otimes \mathbf{n}^i$ along with the definition $\langle a \rangle_\pm = \frac{(a \pm |a|)}{2}$. Then, the tensile and compressive part of the energy are given by

$$\Psi_e^\pm(\boldsymbol{\varepsilon}) = \frac{1}{2}\lambda \left\langle \mathrm{tr}(\boldsymbol{\varepsilon}) \right\rangle_\pm^2 + \mu \mathrm{tr}(\boldsymbol{\varepsilon}_\pm^2) \tag{2.7}$$

Using the expressions of the strain energy of the body from eq. (2.6) and the fracture energy from eq. (2.4), the total energy functional in eq. (2.1) can be rewritten as given by

$$\mathsf{E}(\mathbf{u},\phi) = \int_\Omega \left[(1-\phi)^2 + \mathsf{k}\right] \Psi_e^+(\boldsymbol{\varepsilon})\, d\Omega + \int_\Omega \Psi_e^-(\boldsymbol{\varepsilon})\, d\Omega + \int_\Omega \mathscr{G}_c \gamma(\phi, \nabla\phi)\, d\Omega - \int_\Omega \bar{\mathbf{b}} \cdot \mathbf{u}\, d\Omega - \int_{\partial\Omega_t} \bar{\mathbf{t}} \cdot \mathbf{u}\, dA \tag{2.8}$$

Minimizing the total energy functional $\mathsf{E}(\mathbf{u},\phi)$ results in the coupled evolution equations for the displacement field $\mathbf{u}$ and the phase field ϕ written as follows

$$\nabla \cdot \left\{ \left[(1-\phi)^2 + \mathsf{k}\right] \partial_{\boldsymbol{\varepsilon}} \Psi_e^+ + \partial_{\boldsymbol{\varepsilon}} \Psi_e^- \right\} + \boldsymbol{b} = 0 \tag{2.9}$$

$$\left(\frac{1}{l_\phi} + 2\frac{\Psi_e^+}{\mathscr{G}_c} \right) \phi - l_\phi \nabla^2 \phi = 2\frac{\Psi_e^+}{\mathscr{G}_c} \tag{2.10}$$

along with the Newmann type boundary conditions

$$\boldsymbol{\sigma} \cdot \mathbf{n} = \bar{\mathbf{t}} \quad \text{on } \partial\Omega_t \qquad \text{and} \qquad \nabla\phi \cdot \mathbf{n} = 0 \quad \text{on } \partial\Omega \tag{2.11}$$

It should be noted that the tensile part of the elastic energy Ψ_e^+ drives the evolution of the phase field ϕ. However, the form of eq. (2.10) does not ensure that the phase field is monotonically increasing in the loading history. To enforce the irreversibility of the phase field, a history parameter $\mathscr{H}$ was introduced in the work of Miehe et al. [120]. The history parameter represents the maximum value of the tensile part of the elastic energy in the loading history:

$$\mathscr{H}(\mathrm{x},\mathrm{t}) = \max_{\mathrm{t}\in[0,\mathrm{T}]} \Psi_e^+(\boldsymbol{\varepsilon}) \tag{2.12}$$

Replacing the term $\Psi_e^+(\boldsymbol{\varepsilon})$ in eq. (2.10) with the history parameter $\mathscr{H}$, we can rewrite the evolution equation of the phase field as

$$\left(\frac{1}{l_\phi} + \frac{2\mathscr{H}}{\mathscr{G}_c} \right) \phi - l_\phi \nabla^2 \phi = \frac{2\mathscr{H}}{\mathscr{G}_c} \tag{2.13}$$

Hybrid model

We have two primary field variables: the displacement field $\mathbf{u}(x,t)$ and the phase field $\phi(x,t)$. The strong form of the evolution equations for these two fields is given as

$$\nabla\cdot\left\{\left[(1-\phi)^2+k\right]\partial_{\boldsymbol{\varepsilon}}\Psi_e^+ + \partial_{\boldsymbol{\varepsilon}}\Psi_e^-\right\}+\bar{\mathbf{b}}=0 \tag{2.14a}$$

$$\left(\frac{1}{l_\phi}+\frac{2\mathscr{H}}{\mathscr{G}_c}\right)\phi - l_\phi\nabla^2\phi = \frac{2\mathscr{H}}{\mathscr{G}_c} \tag{2.14b}$$

The introduction of the history parameter $\mathscr{H}$ decouples the above equations and enables us to solve them using a robust staggered scheme. However, because of the elastic energy density split in (2.6), eq. (2.14a) is nonlinear, which results in higher computational cost. To overcome this issue, Ambati et al. [121] introduced a hybrid model that uses a linear momentum balance equation but still ensures that the tensile part of the elastic energy density $\Psi_e^+(\boldsymbol{\varepsilon})$ drives the phase field ϕ. The issue of variational inconsistency of the hybrid model, its ability to produce numerically accurate results, and its ability to predict complex crack patterns are discussed in [121]. Using this model, the strong form of the evolution equations can be rewritten as

$$\nabla\cdot\left\{\left[(1-\phi)^2+k\right]\partial_{\boldsymbol{\varepsilon}}\Psi_e\right\}+\bar{\mathbf{b}}=0 \tag{2.15a}$$

$$\left(\frac{1}{l_\phi}+\frac{2\mathscr{H}}{\mathscr{G}_c}\right)\phi - l_\phi\nabla^2\phi = \frac{2\mathscr{H}}{\mathscr{G}_c} \tag{2.15b}$$

with the definition for the history parameter $\mathscr{H}$ in (2.12) still staying the same. Also, at any point x when $\Psi_e^+ < \Psi_e^-$, the phase field ϕ should be set to zero to prevent the crack surface interpenetration. Also, the evolution equation of the phase field ϕ can be recast into the Ginzburg–Landau type equation with a viscosity parameter υ as

$$\upsilon\dot{\phi} = \partial_\phi \mathsf{E} \tag{2.16}$$

which leads to the modified form of evolution equations written as

$$\nabla\cdot\left\{\left[(1-\phi)^2+k\right]\partial_{\boldsymbol{\varepsilon}}\Psi_e\right\}+\bar{\mathbf{b}}=0 \tag{2.17a}$$

$$\left(\frac{1}{l_\phi}+\frac{2\mathscr{H}}{\mathscr{G}_c}\right)\phi - l_\phi\nabla^2\phi + \upsilon\dot{\phi} = \frac{2\mathscr{H}}{\mathscr{G}_c} \tag{2.17b}$$

2.2.2 Natural neighbor Galerkin method

Natural neighbor Galerkin method is a meshless numerical tool for solving the partial differential equations. Like any meshless method, it does not require fixed connectivity information between nodes. In this section, the application of the natural neighbor Galerkin method to solve the phase field equations is presented.

Let us consider a plane in $\mathbb{R}^2$ consisting of a set of distinct nodal points as shown in Figure 2.2. The construction of trial and test functions is based on natural neighbor interpolation. Natural neighbor interpolants are constructed on the basis of the Voronoi tessellation of the domain with scattered nodal points. The Voronoi tessellation partitions the plane into domains associated with each node such that any point in that domain is closer to the nodal point that it is associated with than any other node in the plane. These domains are called Voronoi or Thiessen polygons. The Voronoi tessellation is unique for a nodal set. Mathematically, Voronoi polygon associated with any node P_I is written as

$$V_I = \{\mathbf{x} \in \mathbb{R}^2 : \ d(\mathbf{x}, P_I) < d(\mathbf{x}, P_J), \ \ \forall J \neq I\} \tag{2.18}$$

where, $d(\mathbf{x}, P_I)$, the Euclidean metric, is the distance between $\mathbf{x}$ and P_I. Any two nodes sharing a common Voronoi edge are called natural neighbors.

Delaunay triangulation of a nodal set is constructed by joining all the natural neighbors. The significance of the Delaunay triangles in this approach is that they are used as the background cells for numerical integration. One of the important properties of Delaunay triangles is the empty circumcircle criterion: the circumcircle of a Delaunay triangle contains no other nodes except the three nodes that form the vertex of that Delaunay triangle. This criterion is employed in finding the nodes that are natural neighbors to any quadrature point. Voronoi Tessellation and Delaunay triangulation of a nodal point set are dual to each other. Voronoi tessellation and Delaunay triangulation for a nodal point set are given pictorially in Figure 2.2(a) and Figure 2.2(b), respectively.

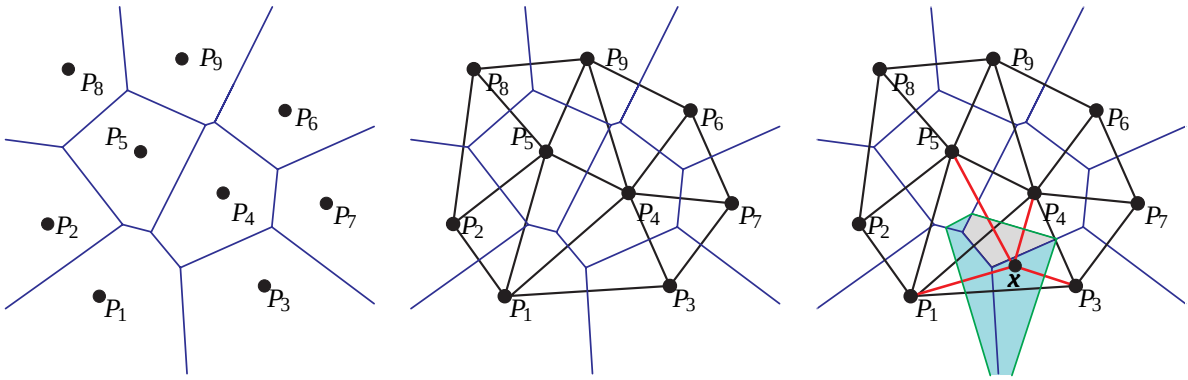

(a) (b) (c)

Figure 2.2: (a) Voronoi diagram of a nodal set, (b) Delaunay triangulation, and (c) Second order Voronoi polygon for $\mathbf{x}$ in the nodal set, indicating the pictorial representation of the shape function computation

A point $\mathbf{x}$ is introduced in the plane consisting of the nodal points at which the natural neighbor interpolant is to be constructed. The empty circumcircle criterion is used to find all the neighbors for the point $\mathbf{x}$. The perpendicular bisectors of all the lines joining the point $\mathbf{x}$ with its neighbors will form a Voronoi cell corresponding to $\mathbf{x}$ (i.e., $V_\mathbf{x}$). The construction of the natural neighbor interpolant at the point $\mathbf{x}$ is based on the definition of second order Voronoi polygon $V_{\mathbf{x}I}$. Mathematically, this second order Voronoi polygon corresponding to $\mathbf{x}$ is written as,

$$V_{\mathbf{x}I} = \{\mathbf{x} \in \mathbb{R}^2 : \ d(\mathbf{x}, P_I) < d(\mathbf{x}, P_J) < d(\mathbf{x}, P_K), \ \ \forall K \neq I, J\} \tag{2.19}$$

This second order voronoi polygon $V_{\mathbf{x}I}$ contains all the points that have P_I as the closest node and P_J as the second closest node. The $\mathscr{C}^0$-continuous natural neighbor interpolant $\mathrm{N}_I(\mathbf{x})$ with respect to node I evaluated at the point $\mathbf{x}$ is defined as the ratio of the area of $V_{\mathbf{x}I}$ to the area $V_\mathbf{x}$. Let us take $\kappa_I(\mathbf{x})$ and $\kappa(\mathbf{x})$ as the Lebesgue measures of $V_{\mathbf{x}I}$ and $V_\mathbf{x}$, respectively. Then, $\mathrm{N}_I(\mathbf{x})$ is given as

$$\mathrm{N}_I(\mathbf{x}) = \frac{\kappa_I(\mathbf{x})}{\kappa(\mathbf{x})} \tag{2.20}$$